Chapter 6

Coherent control of alkali dimers with phase, amplitude, and polarization shaped pulses

In the previous chapters two schemes of independent control over the spectral phase, amplitude, and polarization were presented. In Chapter 4 the genetic algorithm capacities of recognizing the newly gained potential were tested by executing optimizations of the transmission through a rotated polarizer and the efficiency of the second harmonic generation. All that was an introduction to more sophisticated experiments, where the outcomes are not obvious. This chapter covers the issue of coherent control on alkali dimers.

The vectorial features of an electromagnetic field makes it possible to choose an optimal ionization scenario involving the transitions with perpendicular dipole moments, thus demanding different polarizations of the involved photons [78]. Yet, access to the phase and polarization as well as the amplitude of the fs pulse enables even a broader control of the ionization process [83].

The first Sections comment on the choice of the molecular system selected for the experiments and summarize the advantages of the used molecular beam technique. The following Section treats the concept of closed loop experiments and the evolutionary strategies. Next, the experimental conditions are discussed and the influence of various parameters of the fs pulses on the ionization process. Then, the ionization probability is analyzed for a few simple cases of polarized pulses interacting with an ensemble of molecules

with an uniform distribution of the orientation. Finally, the optimal pulse structures are presented and discussed.

6.1 The sodium potassium molecule

Sodium and potassium are both alkali metals found in group one of the periodic table. This means they both have only one electron in their outer shell, which can be very easy contributed to an ionic bound and makes them highly reactive. This simple electronic structure of alkalis is one of the reasons for our interest in the sodium potassium dimer.

Another interesting property of this dimer is the distribution of the vibrational states. The energy gap between the ground and the first excited state lies perfectly within the bandwidth of the Ti:sapphire systems. Moreover, from the first excited state ionization can be obtained by a two photon process. Due to this feature the wavelength conversion is redundant, which makes the optical part of the experiment simpler to realize and therefore more reliable.

The sodium potassium alloy at the room temperature is a silver colored metallic liquid. The boiling temperature is 785°C, which is very convenient when it comes to molecular beam experiments because it allows for producing molecular beam with lower temperature in the apparatus.

The NaK dimers were investigated in our group by means of pump probe spectroscopy [84] and coherent control [85, 86, 87, 88, 89, 90]. The previous experiments did not include polarization manipulation, so continuing the work on a molecule which many features are known seems to be reasonable.

6.2 Molecular beam apparatus

The investigated dimers need to be created in an isolated surrounding, that does not allow them to react with other species or with themselves. For simplicity of the experiment, it is also important to produce them in the vibrational ground state and, to eliminate or minimize the Doppler broadening of the spectral lines, possibly in an arrangement that will minimize the problems arising from their thermal movements. A molecular beam technique

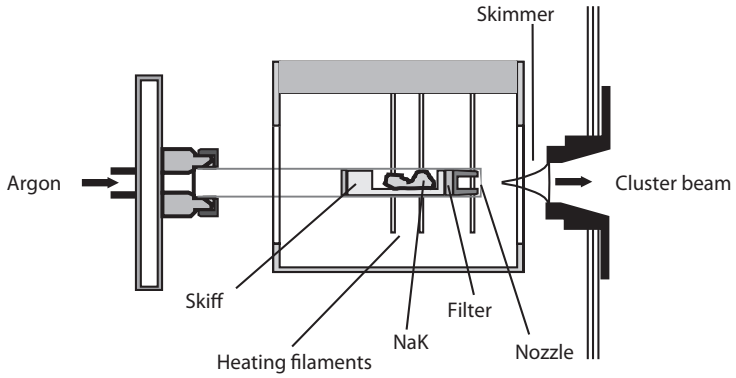

Figure 6.1: The figure presents the oven construction. The NaK as a sample, heating filaments, the nozzle, and the skimmer are indicated as well as the entry point of argon and the outlet of the molecular beam.

meets the above mentioned criteria quite well, therefore we used it in order to investigate the features of the alkalis.

A molecular beam is produced by allowing the alkali vapors to enter the vacuum chamber from a cylinder containing the alloy through a small hole (nozzle). The cylinder containing the alloy is called oven and is heated to approximately 550°C by tungsten heating filaments, as it is presented on Figure 6.1. The molecules which are formed from the resulting vapor of the alloy escape the oven through the $80\,\mu m$ nozzle with argon as a carrier gas and enter the first vacuum chamber called oven chamber. At the high pressure of the carrier gas ($p \approx 2$ bars in this case) the molecules are forming a jet outside the nozzle. Additionally, through collisions with the argon, a majority of them is "cooled" down to the vibrational ground level. Next, from the conical emission of the molecules outside the oven, the beam is formed by skimming off the molecules that travel in directions other than towards the detection vacuum chamber. Afterwards, the molecular beam is crossed with the fs laser beam in the region where the created ions can be extracted by ion optics. The mass of the ionized molecules is selected by a quadrupole mass spectrometer, detected by a secondary electron multiplier and serves as a molecular signal.

To conclude, the highly reactive alkalis are well isolated in vacuum of the molecular beam machine, they are prepared mostly in the ground state

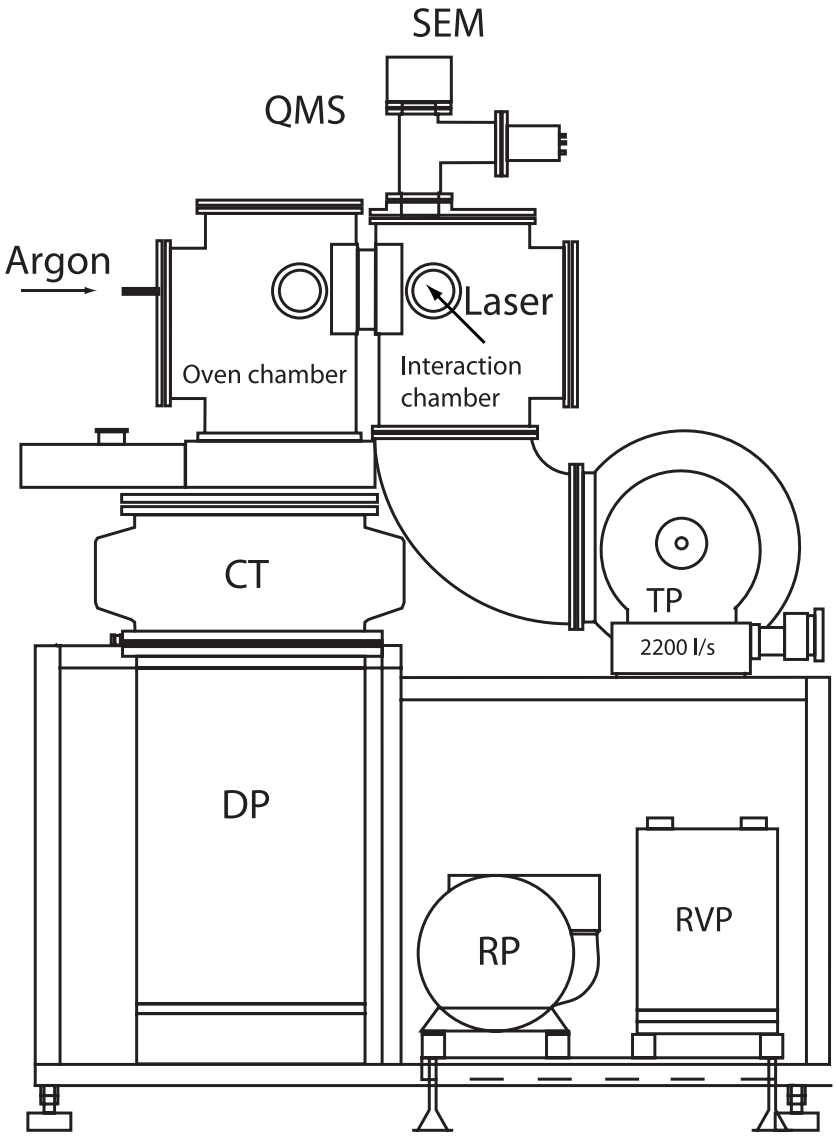

Figure 6.2: The figure presents the molecular beam apparatus with the pointed chambers and vacuum pumps. Pre-vacuum is generated by a rotary van pump (RVP) and a roots pump (RP). A diffusion oil pump (DP) is used to pump the oven chamber and in order to isolate the oil from the chamber, a cooled trap (CT) is placed between DP and the oven chamber. The turbo molecular pump TP is used to pump the interaction chamber. The ionized molecules are detected and mass selected by a QMS (quadrupole mass spectrometer) and a SEM (secondary electron multiplier).

and the Doppler effects are minimized by choice of the geometry of the laser interaction. A detailed description of the molecular beam apparatus can be found in [91].

6.3 Closed loop experiment

The design of an optimal field interacting with quantum mechanical systems in order to succeed with the desired goals is very challenging. There are two ways to approach the problem.

The first one is to calculate the required field. At the start the Hamiltonian of the system has to be found, which alone is a demanding task which will complicate itself tremendously with the complexity of the system. Assuming that the Hamiltonian is known it does not include the information about the optimal field, so still sophisticated calculations of the optimal field have to be performed. Afterwards comes the problem of the experimental generation of the exact field and then delivering it to our system without distorting it. Efforts to achieve the optimal field in this way seems to be time consuming and unpromising.

Another method would be to simply guess the optimal solution. At first it appears to be unreasonable but in practice a well designed trial and error algorithm manages to find the optimal solution relatively fast at the same time escaping the problems of the above mentioned method. Such an approach was first proposed by Rabitz et al. [33, 92, 93, 94]. A quantum mechanical system is regarded there as an analog computer, which by interacting with the field solves the Schrodinger equation instantly. The learning algorithm evaluates the solutions directly on the system and by a trial and error procedure follows the path to the optimal electric field.

The simplicity of this idea allows to avoid complicated and time consuming calculations, as the molecule itself evaluates the quality of the trial solutions. This as well eliminates the problem of generating and delivering the specifically designed field structures.

The learning algorithm tests at first a number of randomly chosen trial pulses on the system, determines the quality of them and based on this information generates a new set of trial pulses. As the algorithm gathers

information throughout the iterations, it eventually learns how to direct the system into the chosen target state.

So far this approach has proved to be very successful. It allowed to control of over 50 molecular systems and other optical processes. In particular one can mention the molecular electronic population transfer [95, 96, 97], control of angular momentum states [98] to photochemistry [99, 100, 101, 102, 103, 104], investigation of biological systems [105, 106], manipulation of quantum wells [107, 108, 109, 110], nonlinear processes like high harmonic generation [111, 112, 113], pulse propagation in optical fibers [114, 115, 116], and chirp control in amplifier systems [117, 30, 118].

In most of those experiments the algorithm used is based on Evolutionary Algorithms (EA). Details of the EA [119, 120] can vary slightly depending on the system to be optimized, but generally they will not be much different. The EA used for those experiments is discussed in [58, 76] and it can be divided into initialization and loop.

At the initialization first a set of 10 individuals is created. The properties like the phase, transmission, and polarization of modulators pixels of each individual, considered as genes, are chosen randomly. The loop is a part of the algorithm, which is performed iteratively until the satisfactory output is reached.

At first by a repeated recombination 30 offsprings are created from the parent population. The process takes two random parents and interchanges the genetic material between them and creates new individuals.

Next comes mutation which modifies the genes of the offsprings from the ones inherited from their parents. Generally, this is done by adding a random number from a gaussian distribution of standard distribution σ and mean expectation value equal to zero to the genes. There are various ways to modify σ. Our algorithm is based on the 1/5th rule, which is based on the philosophy of letting the algorithm widen the horizons of the search area when the success rate is larger than 1/5th and narrow them for the opposite case. Broadening the search corresponds to increasing the existing mutation rate by 20% and narrowing is decreasing the mutation rate by 20%.

After recombination and mutation, the algorithm evaluates the population by testing the resulting pulses on the system. The extent to which the

desired goal is realized, or in other words how well the individual has adopted to the environment, is called fitness. During that process all individuals are tested and the corresponding fitness can be assigned.

Finally, at the selection stage, the individuals are sorted by fitness and the 10 best are selected. Then survivors will serve as parents in the next iteration of the loop. Since we chose to include elitism, in the next iteration the best parent will be included in the evaluation stage.

This procedure is executed until the user decides to terminate it which happens when an optimal solution is found or by some reasons no convergence is observed. The second, unfortunate case can occur for dramatical and rapid changes of experimental conditions, for example a stuck nozzle in the molecular beam or laser malfunction.

6.4 Experimental conditions

As mentioned in the first Section of this Chapter, one of the reasons for choosing the sodium potassium molecule is continuing the work of the group on this subject. Previously performed experiments [85, 86, 87, 88] allow to gather important insights about the molecule behavior and also gave us outcomes that we can relate to. The latest experiments were carried out with a regenerative amplifier RegA from Coherent, seeded by a Mira oscillator, which has different specifications then a previously used Tsunami from Spectra Physics.

	Spectra	Coherent
Energy	10nJ	3μJ
Bandwidth	8nm	35nm
Rep. rate	80MHz	300kHz

Since the new system uses an amplifier after the oscillator the energy of the generated pulses is approximately 300 times higher, but still in the regime where the perturbation theory can be applied [121].

The available bandwidth makes it possible to employ transitions unaccessible before in the optimization scheme, so control over the wave packet propagation is improved. Broadening of the spectra allows for a higher opti-

mization factors and since the wave packets consist of additional components, slightly modified optimal pulse structures can be expected.

For 80MHz, the time interval between two incoming pulses is smaller than the travel time of the molecules through the interaction zone. It was previously argued that since the pump probe spectra remains unchanged for 80MHz and 1kHz, the processes in the molecules do not vary when the molecule is irradiated a few times [122]. This is an indication that the same situation is valid when the pulses are shaped and still the state of the molecule is influenced by a single pulse form and not by a sequence of them. In case of 300kHz this problem simply vanishes, because the beam velocity allows for molecules to escape the interaction zone before the following pulse irradiation.

The above described change makes it difficult to compare the optimization factors obtained with the old to the new laser setup. The specifications of the recently used pulses allow for different optimal paths while employing a broader spectrum, higher intensities, and the newly introduced possibility of manipulating the polarization of the electric field. Thus, the old outcome can be exploited as a guidance in interpretation of the new optimal pulse structures.

6.5 Optimal ionization scenario for different types of optimizations

Apart from various laser pulse specifications, the algorithm combined with the serial shaper setup has a new degree of freedom, namely the polarization. Together with the phase and the amplitude, the effect upon the molecular wave packet dynamic is wider.

The available wavelengths within the spectrum of fs pulses allow for addressing various transitions. By modulating the spectral amplitude we are given a choice of diminishing transition probabilities. Optimization of ionization processes is effective when all possible transitions are employed in the process, therefore, in this case, the optimal amplitude is usually close to maximum for the whole spectrum.

Amplitude modulation alone, with the assumption of a flat spectral phase has minimal impact on the temporal pulse shape. By reducing the bandwidth

one can prolong the pulse duration and cutting out spectral components would not lead to a pulse structure different from a single peak. Thus, an amplitude filter can be used to address excited states, but its control over the introduced wave packet dynamics is restrained to the choice of which vibrational states will be involved.

Phase modulation, on the other hand, is a tool to influence the dynamics of the introduced wave packets [123, 124, 125, 126]. The used bandwidth of a fs laser populates many vibrational states of the first excited electronic level. Generated in this way a wave packet is composed of those occupied vibrational states which interfere. In the case of a harmonic potential, the created wave packet would propagate without change of shape, but in a molecular potential, approximated by a Morse potential various processes take place which modify this behavior [127]. Some of them are analogue to dispersion in optical materials. The phase of the wave function of the contributing states is set by the phase of the exciting radiation. This mechanism allows for a phase shaping to optimize the propagation of wavepackets. Already simple chirp control is capable of focusing a wave packet propagating along the energy surface at desired potential coordinates [128]. A more complicated phase modifies the pulse structure and thereby drives the wave packet so the molecule is efficiently ionized.

Shaping of the polarization allows accessing transitions that without this feature would have a very low propabilities. A practical example can be presented by transitions in NaK, displayed in Figure 6.3. The first transition from the ground state $X(1)^1\Sigma^+$ to the first excited state $A(2)^1\Sigma^+$ according to the selection rules requires one photon linearly polarized. Since we assume that the distribution of dimers is homogenous, then any linear polarization will transfer electron population to higher levels for the molecules which were orientated accordingly. For the sake of argumentation let us assume that this first transition is caused by P polarized light, so in this way, a geometrical selection of the molecules has been made by the excitation. Next, the most expected scenario is that the energy gap will be closed between the $A(2)^1\Sigma^+$ and the ionic $X(1)^2\Sigma^+$ state by a two photon transition. Another possibility is to climb the ladder by the intermediate $A(6)^1\Sigma^+$. It has to be emphasized, that since the first transition is $\Sigma \rightarrow \Sigma$ for the linear light polarization the

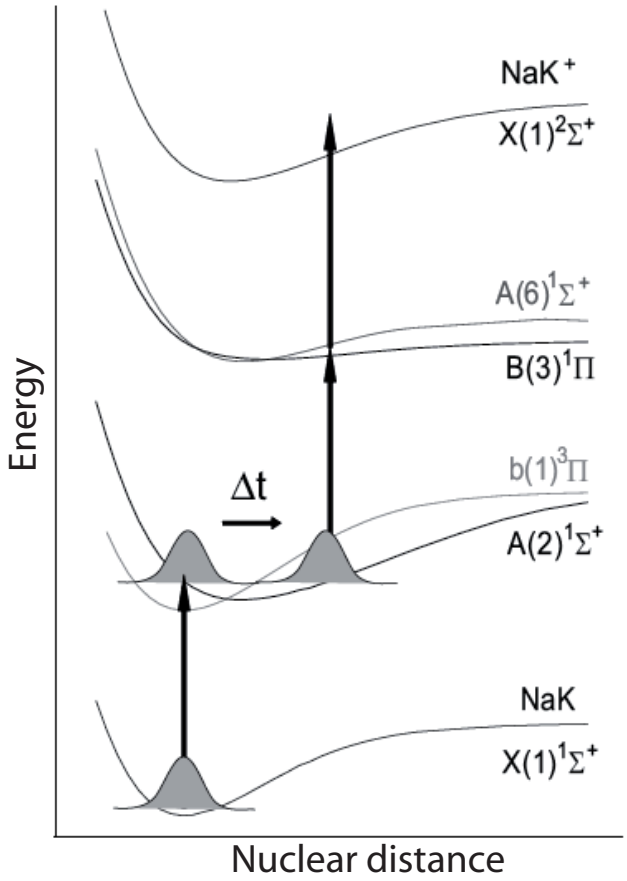

Figure 6.3: Scheme of the involved vibrational potentials of NaK. The most probable transitions are depicted by the arrows.

only allowed transition will go through Σ states. This is not the case when the polarization is optimized as well. The ladder climbing can then be realized by employing the $B(3)^1\Pi$ or $A(6)^1\Sigma^+$ state or both.

Using various polarizations surpasses the limitations to transitions only having parallel transition moments and broadens the choice of the used ionization paths.

6.6 Ionization probability

In the Section above it was mentioned that the orientation of the molecules is assumed to be homogenous. This brings up the question if the manipulation of the polarization makes the ionization process more efficient or if it just opens new paths for the ionization scheme. It is in particular interest if linearly or circularly polarized pulses will excite a higher number of molecules whose angular alignment is equally distributed. Moreover, how does it work for the case of one and two photon transitions?

In order to answer this questions, simple calculations were made concerning the number of potentially excited molecules. The transition probability is proportional the intensity of the electromagnetic field and to the transition dipole moment M_{nm}, which is given by the integral

$$M_{nm} = \int \Psi_n^* \, e\vec{\mu} \Psi_m dr$$

where $e\vec{\mu}$ is an electronic dipole operator. For the chosen states n and m and the proper electromagnetic field polarization, M_{nm} is constant. Now, let us simplify the problem. We assume that the light polarization needed for the transition is linear. Then any light polarization can be described as a superposition of two perpendicularly polarized waves. When one of these waves has a polarization along the desired direction described by selection rules, then the other one has an orthogonal direction, for which the dipole moment is equal zero and it therefore does not contribute to the transition probability. Thus, the intensity that the molecule "sees" is the appropriate polarization component, which is proportional to the square projection of an electrical field vector on the dipole moment vector. In order to visualize this

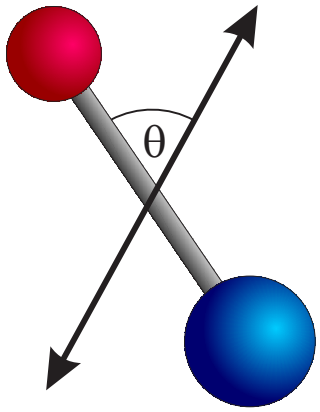

Figure 6.4: NaK molecule relative orientation to linearly polarized light.

situation we will suppose that the dipole moment vector overlaps with the orientation of the molecular axis, as presented on Figure 6.4.

In our simple model, the probability of a single photon excitation if linear polarized light used is described by

$$P_{lin}^{\omega} \sim M_{nm} E_0^2 \cos^2 \theta \tag{6.1}$$

where θ is the angle between the orientation of the molecule axis and light polarization. The molecules orientations are distributed homogenously, therefore the number of the excited ones is yielded by integration over all possible orientations.

$$N_{lin}^{\omega} \sim M_{nm} \int_0^{\pi} E_0^2 \cos^2 \theta d\theta = \frac{\pi}{2} M_{nm} E_0^2 \tag{6.2}$$

For circularly polarized light the situation, as presented in Figure 6.5, is slightly different. The probability is no longer dependent on the relative orientation θ, but only on the intensity. Equal probability does not depend on the orientation of the molecule, since the circular polarization can be analyzed as a superposition of any orthogonally polarized waves of equal amplitudes. Although this feature is very convenient, it also means that while the total intensity remains constant, the intensity "seen" by the molecule is effectively different compared to the linear polarization case.

Since

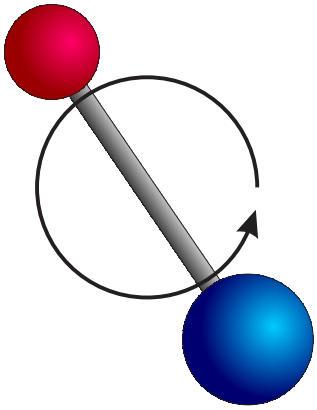

Figure 6.5: NaK molecule interacting with circularly polarized light. As shown, for any given orientation of the molecule it "sees" the same intensity.

$$E_0^2 = E_\perp^2 + E_\parallel^2$$

and for circular polarization $E_\perp = E_\parallel$

$$E_\parallel = \frac{1}{\sqrt{2}} E_0.$$

The effective intensity is equivalent to $E_\parallel^2$ so the probability becomes

$$P_{circ}^{\omega} \sim \frac{1}{2} M_{nm} E_0^2 \,. \tag{6.3}$$

The number of excitations is given by performing Integration 6.4.

$$N_{circ}^{\omega} \sim M_{nm} \int_0^\pi \frac{1}{2} E_0^2 d\theta = \frac{\pi}{2} M_{nm} E_0^2 \tag{6.4}$$

The number of excited molecules with a single-photon process is the same for linear and circular polarization. The difference lies in the orientation distribution of the excited molecules. The interaction with a linearly polarized field selects the molecules with a parallel alignment of their dipole moment, so the excitation can be regarded as a orientation selection, whereas circular light excites all orientations in the same way.

A similar argumentation can be given for the two-photon transition with different dipole transition moments, where the probability is proportional to

the square of the intensity. This leads to the number of excitations for linear polarization

$$N_{lin}^{2\omega} \sim M_{nk} \int_0^{\pi} E_0^4 \cos^4\theta d\theta = \frac{3}{8}\pi M_{nk} E_0^4 \,, \tag{6.5}$$

and for the circular excitation

$$N_{circ}^{2\omega} \sim M_{nk} \int_0^{\pi} \frac{1}{4} E_0^4 d\theta = \frac{1}{4}\pi M_{nk} E_0^4 \,. \tag{6.6}$$

There is a 50% higher number of excitations in two photon process for linear pulses, even though the molecular orientation is equally distributed.

The NaK dimer needs three photons at 780nm for the effective ionization. Starting with the first single-photon transition having circular polarization the same number of molecules are excited as in the case of a linearly polarized photon, but for the latter, the excited molecules will be orientated. Working with an ensemble of molecules with a preselected orientation makes the efficiency of the next excitations higher with linear polarization.

It appears that from the first excited state $A(2)^1\Sigma^+$, it is much more efficient to use a linear light polarization to transfer the population to the ionic state instead of circular polarization. This difference will be even more pronounced when we select the orientation of the molecules with the first transition to $A(2)^1\Sigma^+$. Now, the two photon transition to the ionic state could be realized through the intermediate $B(3)^1\Pi$ state or the $A(6)^1\Sigma^+$. The dipole moments of these transitions are orthogonal, so polarization shaping becomes very effective at this point.

6.7 Optimal pulses

The NaK dimers were ionized by pulses whose different combinations of parameters were optimized. With the serial shaper setup it was possible to choose the parameters which were optimized, as it was previously described in Section 4.5. From the seven possible combinations three types of optimizations have been chosen to be employed in this experiment: spectral phase optimization (PXX), the phase and the amplitude (PXP), and ultimately the phase, the amplitude, and the polarization (PAP).

In previous experiments done with the Tsunami oscillator [85, 86, 87, 88, 89] where ionization was the goal, the amplitude shaping contrary to the phase modulation did not contribute significantly to process efficiency, but prolonged the convergence time. It can be interpreted that the additional spectrum components do not interrupt the wavepacket propagation whereas a lack of vital components will decrease the ionization rates. Thus, only phase was manipulated in order to increase the ionization and phase and amplitude optimization were discarded. The same policy was applied for the experiments including the new laser system.

As a new reference for the spectrally broader and energetically higher pulses a few PXX optimizations were performed. Forming the spectral phase, in a simple explanation, is capable of controlling the wavepacket propagation. The most expected scenario is to transfer the electron population with a first sub-pulse to the first excited state $A(2)^1\Sigma^+$. Additionally, it is possible through phase shaping to focus a created wavepacket [129] at the outer turning point, where the Franck-Condon factor is favorable and thus the transition probability for a two photon ionization is higher. The ionization can be achieved by a second sub pulse delayed by $(n + \frac{1}{2})T$, where $T = 440$ fs is the period of the wave packet oscillation on the $A(2)^1\Sigma^+$ state [84]. For the narrow bandwidth pulses their duration makes it difficult to resolve 220 fs half period and the sub-pulse temporal separation corresponding to 1.5 oscillations is observed [85]. Additionally, using the narrow spectrum offers less control over the wave packet dynamics. With the RegA pulse bandwidth of FWHM$\geq$30nm the temporal resolution is in the range that permits the ionization after half of the oscillation period with the separated sub-pulse.

An optimal pulse structure with its spectrum for the performed PXX optimization is presented in Figure 6.6.

In the temporal picture, instead of two pulses we observe three sub pulses with separations of 380 fs and 280 fs. This structure indicates a sequential ionization process within one pulse form, but the sub pulse separation do not support the above mentioned model of subsequent excitation and ionization for following sub pulses. The separation between the first sub pulse and the second cannot be interpreted as half of the period of the wave packet oscillation on the $A(2)^1\Sigma^+$ and therefore, due to the Franck-Condon princi-

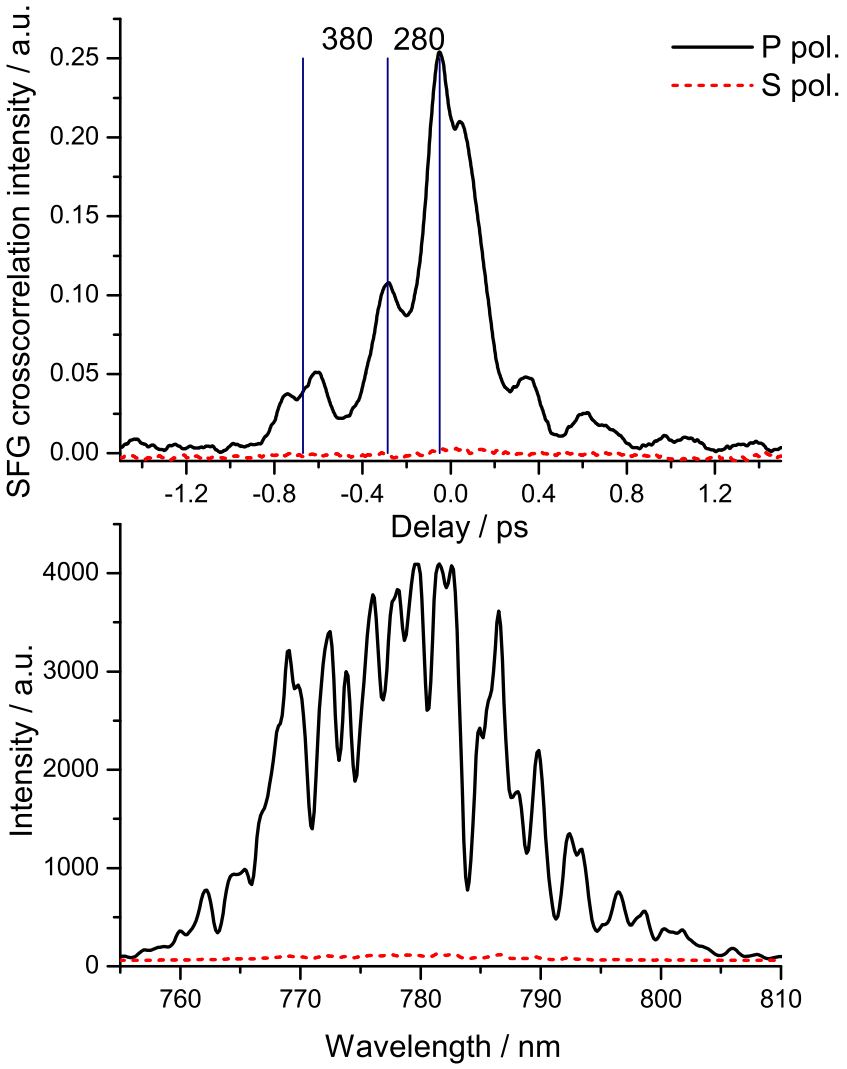

Figure 6.6: Pulse structure obtained in a PXX optimization. The upper graph presents the crosscorrelation recorded in the P and S plane, indicated by black and red dashed lines respectively, with temporal separations of the sub pulses displayed. The lower graph shows the spectra for the P and S directions of polarization.

ple [130], the ionization by the second sub pulse which comes 380 fs later is highly improbable. Interestingly, the distance between the first and the third sub pulse is 660fs, which is equal to 1.5T. Furthermore, the temporal separation between second and third sub pulse is close to 0.5T. It may suggest a few plausible ionization schemes, but to properly understand the processes leading to the optimal ionization a more detailed and theoretical analysis is required.

The second intriguing feature in Figure 6.6 is the spectrum. The P component is modulated, which seems odd at first. One could expect that the phase only modulation should leave the spectrum intact and the spectrum modulation comes from improper modulator calibration. On the contrary, for a random spectral phase, a modulation of the spectrum occurs despite of calibration quality. It originates from the interference of phases written from neighboring pixels, where the parts of the pixels bandwidths overlap. For the phase difference equal to π, the two waves interfere and cancel themselves out.

Next, a PXP pulse optimization was run. Apart from the above mentioned impact that the phase of the pulse has on the wavepacket propagation, the optimal path of the ionization can now employ transitions that require different transition moments. This effectively broadens the accessible ionization schemes by the simple fact that in this optimization, by proper choice of polarization, $\Sigma \rightarrow \Sigma$ or $\Sigma \rightarrow \Pi$ transitions can be used. The temporal pulse structure displayed on the upper graph in Figure 6.7 shows the temporal evolution of the pulse corresponding to PXP optimization. One can recognize two strong, and three weak sub pulses there. The separation between the two strongest orthogonally polarized pulses amounts to 610 fs, which can be interpreted as 1.5T. The weak sub pulses are as well organized in a rather regular structure where the separations are close to $\frac{1}{2}T$ and the relative polarizations are orthogonal. This suggests again a sort of a sequential process, but since many more transitions can contribute, one can only speculate without suitable theoretical calculations of polarization shaping.

The spectra of the optimal pulse show the alternating of the peaks for the P and S spectra. When we exclude the interferometric effects described in case of PXX, this feature can be explained from the fact that for PXP

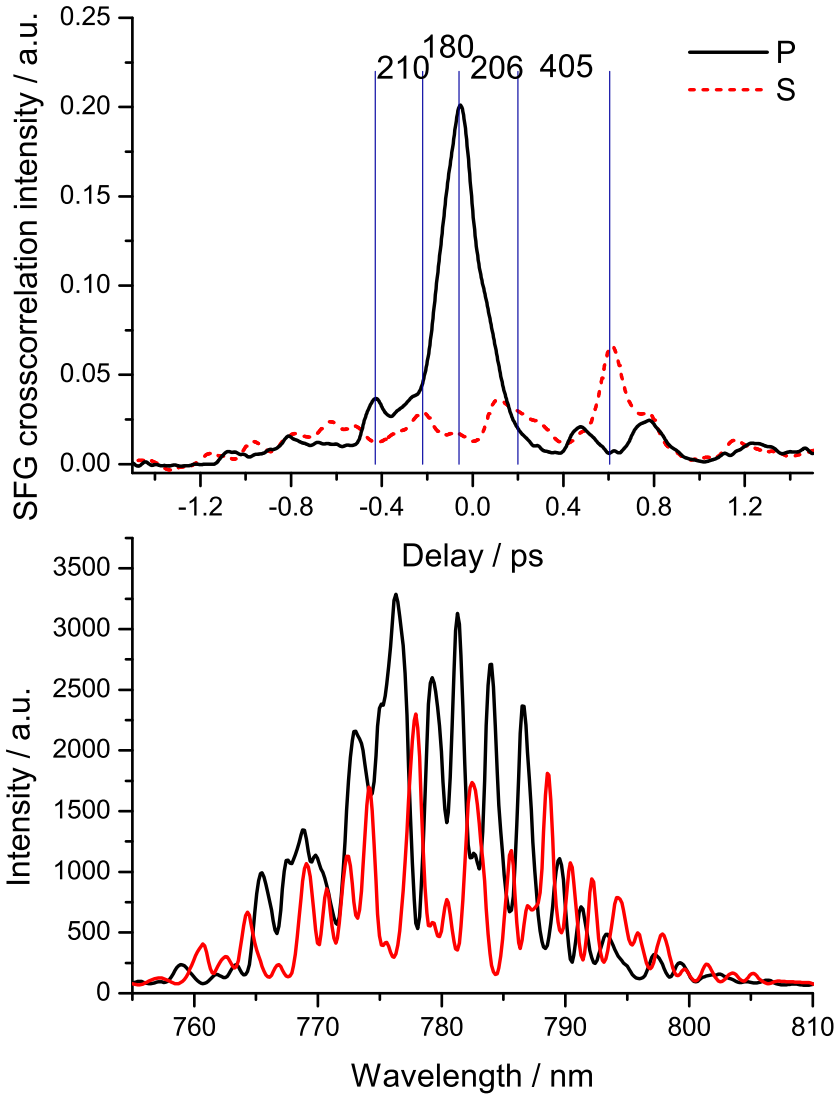

Figure 6.7: Pulse structure obtained in a PXP optimization.

shaping, the spectra summed together should give the incoming spectrum of an unshaped pulse. Polarization shaping of in this case can be regarded as dividing the intensity between the P and S direction. Because of this effect it is hard to point at the spectral components, P or S, that are actually responsible for any processes, while they can only be present there for the reason that a lack of the same spectral components was required in the orthogonal spectrum. Since the efficiency of this type of optimization is distinctly higher in comparison with PXX, the PXP optimization is most probably not the case of eliminating the unwanted frequencies, but it is difficult to exclude this possibility.

The last type of optimization performed was PAP, which controls all parameters accessible by the serial shaper. In addition to PXX and PXP, in this type of optimization the algorithm can decide to cut a few frequencies out, if they interfere with the optimal ionization path. The pulse structure obtained for the PAP optimization of the NaK ionization is shown in Figure 6.8.

The temporal structure shows remarkable features. The sub pulses are organized in almost equal distances of 220 fs and their relative polarizations are perpendicular. This is a beautiful and very strong manifestation of the previously discussed sequential model of ionization. It is also interesting, that the pulse structure ends with a circularly polarized pulse. The difference to the PXP optimization is that realizing such a pulse structure is slightly less difficult when the amplitude is modulated.

A brief examination of the spectra shows no indications of the alternating peaks effect present in the PXP optimization. The spectral polarization can be chosen here independent of the amplitude.

In order to compare the presented optimizations the obtained optimization factors are exhibited in Figure 6.9. The expansion of search space by including the polarization has a noticeable influence on the efficiency. Optimizations of the phase resulted in almost 180% of the signal in relation to one generated by a short pulse, whereas for the polarization and phase optimization factors reached 207%. The change between the PXP and PAP is not as stunning as the difference between PXX and PXP, but there is certain increase to almost 220%. This is not very surprising, since it was

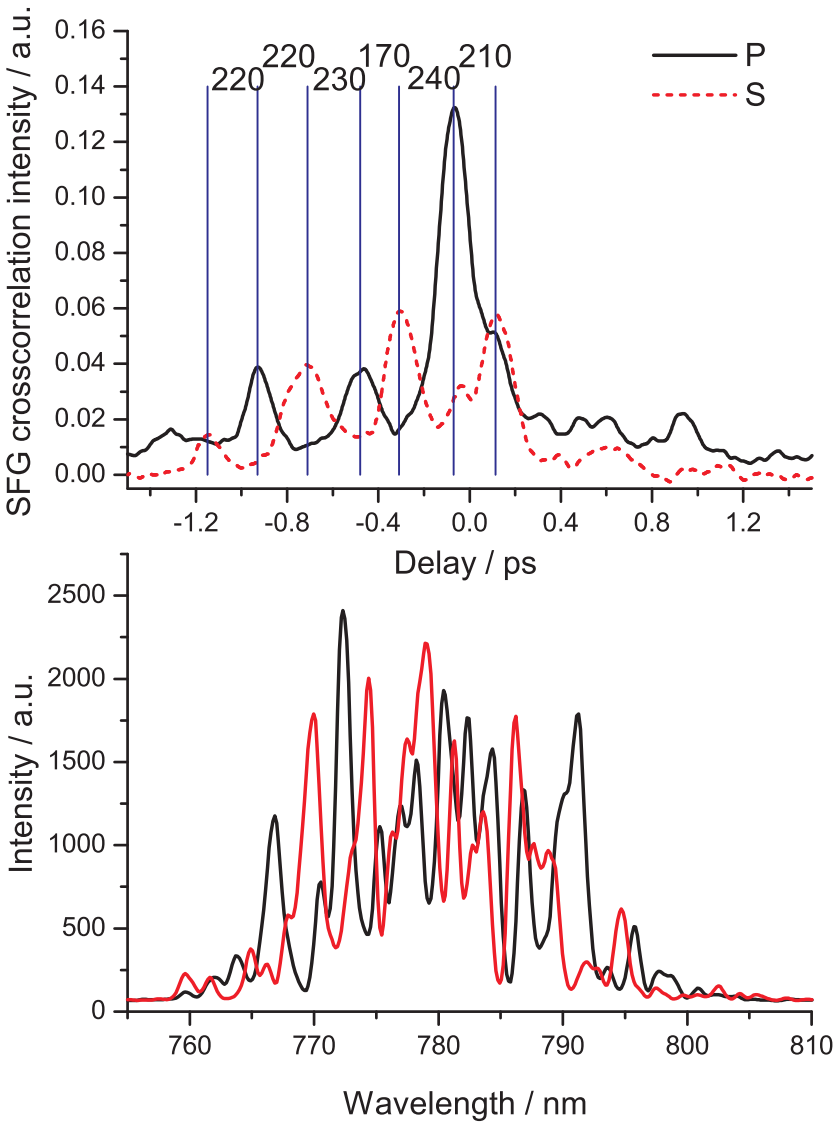

Figure 6.8: Pulse structure obtained in a PAP optimization.

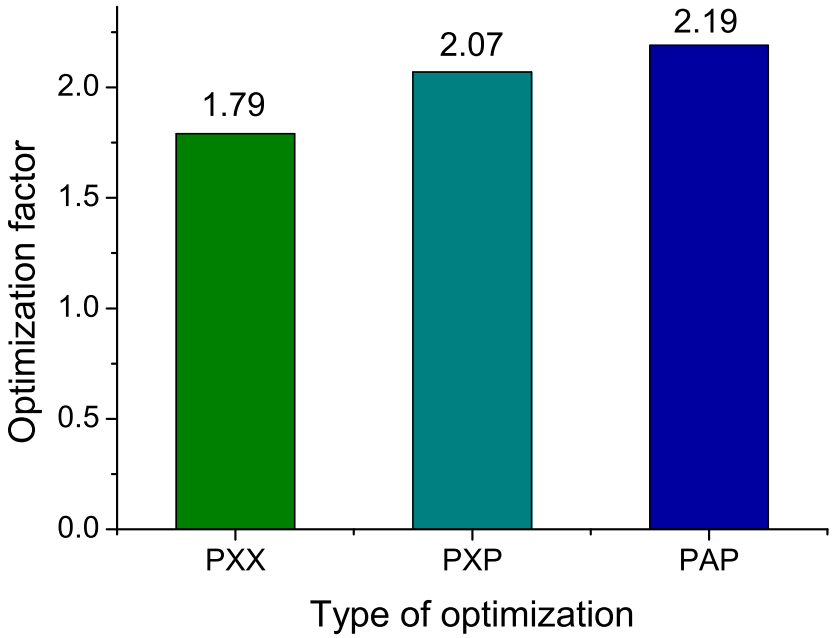

Figure 6.9: Comparison of the optimization factors for different types of optimizations.

observed that in case of ionization, including the amplitude modulation does not have a dramatic influence on the efficiency. The actual impact of hindering of the undesired frequencies could be much better observed in enhancing of the selective ionization, where one of the species is maximized and others minimized. An example of such experiment is an isotope ratio optimization [88, 131].

Nevertheless, the factor change proves that even simple diatomic molecule processes like ionization can be tremendously influenced by the use of phase, amplitude, and polarization shaped pulses.

6.8 Summary

In this chapter coherent control experiments on the NaK dimer were described and discussed. By comparing the ion yields obtained in the three

types of optimization, where first the phase alone, then the phase together with the polarization and finally all parameters including the amplitude were manipulated, it was shown that the ability to address the transitions with perpendicular and parallel dipole moments sufficiently raised the efficiency of the process. The pulse structures provided by the optimizations support the concept of sequential ladder climbing on the potential energy surfaces. The introduction of polarization changes that scenario in a way, that the following sub pulses have perpendicular polarization with respect to each other, which is a strong indication of employing $\Sigma \rightarrow \Sigma$ and $\Sigma \rightarrow \Pi$ transition in the process as well.